JOURNAL OF MATERIALS SCIENCE 30 (1995) 1977–1981

A composite model for superplasticity

B. BAUDELET, JIANSHE LIAN*
Génie Physique et Mécanique des Matériaux, Unité Associée au CNRS ENSPG, Institut National Polytechnique de Grenoble BP46, 38402, Saint Martin d'Hères, France

A composite model for superplasticity, based on the joint influences of both the behaviour of a composite boundary and creep, is proposed. In this model, superplasticity is considered as a combination of two mechanisms: grain-boundary sliding and dislocation creep, which occur either together or sequentially. Applied to experimental data, it can describe the logarithmic stress versus strain rate curves observed for superplastic materials showing regions I, II and III.

1. Introduction

In the last two or three decades, a number of mechanism models have been proposed to clarify the dominant microstructural features of superplasticity [1–9]. Both theoretical models and microstructural observations indicate that the most important feature of superplasticity is the role played by grain-boundary sliding (GBS). However, dislocation motion or diffusion in grains or near-grain-boundary regions must always be invoked to maintain a continuous superplastic deformation. Consequently, most models consider superplastic deformation as a GBS process associated with and rate controlled by the accommodation processes, i.e. the diffusion-accommodation model of Ashby and Verrall [3], and the dislocation pile-up accommodation models of Ball and Hutchinson [4] (Fig. 1a) and Mukherjee [5].

The typical superplastic mechanical behaviour is represented by the log σ versus log $\dot{\varepsilon}$ curve which can be divided into three regions I, II and III. Superplasticity occurs in region II with a high strain-rate sensitivity, $m(m \geqslant 0.5)$ while in regions I and III, the strain-rate sensitivity values are about 0.2–0.3. To account for this typical behaviour, the phenomenological transition model was proposed by Hart [10]. The high strain-rate sensitivity behaviour can be simulated by applying the numerical finite element method to the creep constitutive law of polycrystalline materials affected by the Newtonian grain-boundary sliding [11, 12]. The behaviour can be represented by

$$\dot{\varepsilon} = \alpha_2(f\sigma)^n$$

or

$$\sigma = \frac{1}{f} A_2(\dot{\varepsilon})^{1/n} \quad (1a)$$

$$= \frac{1}{f}\sigma_a(\dot{\varepsilon}) \quad (1b)$$

where $\dot{\varepsilon}$ and σ are, respectively, the applied strain rate and stress, $\sigma_a(\dot{\varepsilon})$ is the constitutive law for dislocation creep, n is a stress-sensitivity exponent which is about 4–5 for dislocation creep, α_2 and $A_2(=(1/\alpha_2)^{1/n})$, are constants, and f is the transition parameter which is greater than one when grain-boundary sliding takes place.

This expression, obtained by numerical analysis, was also deduced from a composite boundary model [13]. In the composite boundary, formed by grain boundaries and their band prolongations inside the grains (Fig. 1 in [13]), shear bands can develop. In this model, f is greater than 1 and is a topological function because its value increases for composite boundaries with a high grain-boundary fraction. This composite boundary model is similar to those previously proposed [4]. This mechanism was experimentally observed [14–16].

The composite boundary model [13] ascribes the observed deformation behaviour in a sequence of controlling mechanisms. Region I is characterized by creep inside the grains which controls the deformation of the composite boundary. The transition from region I to region II reflects the progressive transfer of control to the behaviour of the grain boundary which is accompanied by the development of increasingly wider shear bands in the grains. The composite boundary-controlled deformation in region II is progressively replaced by an overall creep in the material to reach, finally, region III in which the composite boundary completely loses its influence.

2. Analysis

2.1. The composite model for superplasticity

From the composite boundary model, the average applied stress is defined as

$$(a + b)\sigma(\dot{\varepsilon}) = a\sigma_a(\dot{\varepsilon}) + b\sigma_b(\dot{\varepsilon}) \quad (2)$$

where $\sigma_a(\dot{\varepsilon})$ and $\sigma_b(\dot{\varepsilon})$ are the stresses for dislocation creep and gain-boundary sliding, respectively. The

* *Permanent address*: Department of Metal Materials Engineering, Jilin University of Technology, Changchun, 130025, People's Republic of China.

0022–2461

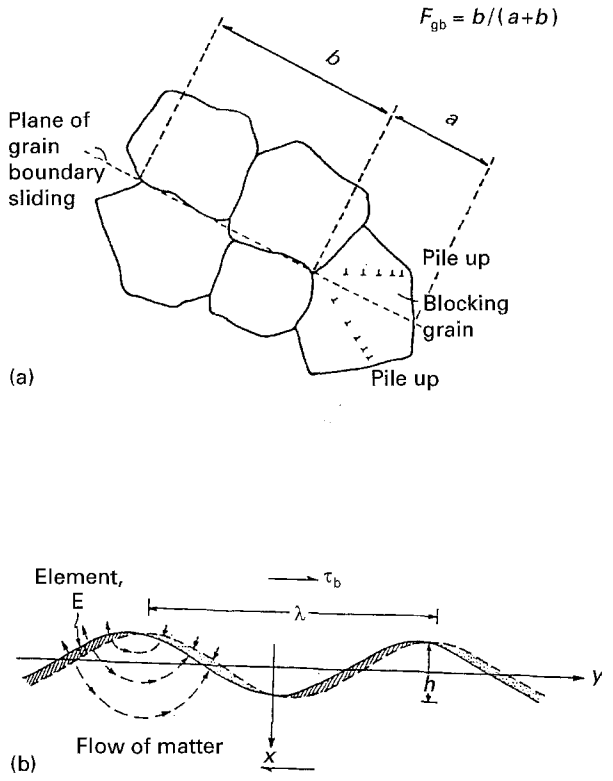

Figure 1 (a) Schematic illustration of dislocation slip acccommodation in the grain-boundary sliding model of Ball and Hutchinson. (b) Grain boundary sliding described by Raj and Ashby.

definitions of the surfaces a and b are shown in Fig. 1. Equation can be rewritten as

$$\sigma(\dot{\varepsilon}) = (1 - F_{gb})\sigma_a(\dot{\varepsilon}) + F_{gb}\sigma_b(\dot{\varepsilon}) = \frac{1}{f}\sigma_a(\dot{\varepsilon}) \quad (3)$$

where $F_{gb} = b/(a + b)$ is the fraction of the stress contribution due to grain-boundary sliding. Introducing Equation 1 in Equation 3 gives the expression for f

$$f = \frac{1}{1 - F_{gb}(1 - \sigma_b/\sigma_a)} \quad (4)$$

Equation 1 with Equation 4 is the modified expression for the Baudelet model [13]. In the above derivation, the equal-strain rate, i.e. the Taylor assumption, was used. This model is applicable to the case where the applied stress is smaller than the flow stress for dislocation creep (regions I and II); it can describe the transition behaviour from region I to region II fairly well. However, at the higher strain rates in region III, or towards the end of region II, the model always overestimates the flow stress. Fortunately, the Ashby and Verrall (A–V) model [3] can describe the transition behaviour from region II to region III. Following the A–V model, we therefore assume that the total strain rate can be expressed as

$$\dot{\varepsilon} = \alpha_2(f\sigma)^n + \alpha_2\sigma^n = (1 + f^n)\alpha_2\sigma^n \quad (5a)$$

or

$$\sigma = A_2\left(\frac{\dot{\varepsilon}}{1 + f^n}\right)^{1/n} \quad (5b)$$

Equation 5a and b, where f is expressed by Equation 4, are the expressions for the composite model for superplasticity based on both the Baudelet and the A–V concepts.

2.2. Grain-boundary sliding and dislocation creep

The Raj and Ashby model [7] describes grain-boundary sliding and is schematically illustrated in Fig. 1b. According to the model, the displacement rate, $\dot{U}$, for a steady-state sliding of a sinusoidal boundary with local diffusion accommodation, is expressed as

$$\dot{U} = \frac{8\lambda\Omega}{\pi kTh^2} D_v\left(1 + \frac{\pi\delta D_{gb}}{\lambda D_v}\right)\tau_b \quad (6)$$

where Ω is the atomic volume, δ the grain boundary width, h and λ the amplitude and wavelength of the sinusoidal curved grain boundary, respectively, and kT has the usual meaning. $D_{gb} = D_{gb0}/\exp(-Q_{gb}/RT)$ and D_v are the grain-boundary and volume-diffusion coefficients, respectively, Q_{gb}, the activation energy for grain-boundary diffusion, D_{gb0}, the pre-exponential factor, R the gas constant, and τ_b, the shear stress for grain-boundary sliding. For small grain sizes, $\pi\delta D_{gb}/\lambda D_v \gg 1$, and Equation 6 becomes approximately

$$\dot{U} \approx \frac{8\Omega\delta D_{gb}}{kTh^2}\tau_b \quad (7)$$

Using $\dot{\gamma} \approx 2\dot{U}/d$ and $\Omega = \boldsymbol{b}^3$, where $\boldsymbol{b}$ is the Burgers vector, and assuming that h is proportional to d, one obtains

$$\tau_b = A_1^*\frac{kT}{\delta D_{gb}}\left(\frac{d}{\boldsymbol{b}}\right)^3\dot{\gamma} \quad (8a)$$

$$\sigma_b = A_1\frac{kT}{\delta D_{gb}}\left(\frac{d}{\boldsymbol{b}}\right)^3\dot{\varepsilon} \quad (8b)$$

where A_1 and A_1^* are adjustable material-dependent constants. This is the expression for grain-boundary sliding accommodated by local diffusion based on the Raj and Ashby model. One notes that the Coble creep is described in a similar way.

The stress for dislocation creep can be expressed through an empirical relationship

$$\sigma_a = A_2^*\left[\frac{kT}{D_0\exp(-Q/RT)}\dot{\varepsilon}\right]^{1/n} \quad (9a)$$

This can be simplified to

$$\sigma_a = A_2(\dot{\varepsilon})^{1/n} \quad (9b)$$

where D_0 is the pre-exponential factor and Q the activation energy, which may be either for volume diffusion or for grain-boundary diffusion. A_2 and A_2^* are adjustable material-dependent constants.

By introducing Equations 8b and 9b into Equation 4, one finally obtains the expression for the presently proposed composite model for superplasticity

$$\sigma = A_2\left(\frac{\dot{\varepsilon}}{1 + f^n}\right)^{1/n} \quad (10a)$$

where

$$f = \left\{1 - F_{gb}\left[1 - \frac{A_1 kT}{A_2 \delta D_{gb}}\left(\frac{d}{b}\right)^3 (\dot{\varepsilon})^{1-1/n}\right]\right\}^{-1} \quad (10b)$$

3. Application

3.1. Zn–22% Al alloy

Zn–22% Al is a typical superplastic alloy. The log σ versus log $\dot{\varepsilon}$ data points [17] of this alloy with a grain size $d = 2.5\,\mu m$ are plotted in Fig. 2 for three test temperatures: 423, 473 and 503 K. For the same temperatures, the composite model predicts the behaviour shown by the solid lines when the parameters in Table I are used. Both A_1 and A_2 are fitting parameters; A_2 was adjusted to fit the data for each temperature. Apart from A_2 (see Table II), all the parameter values are independent of the test temperature. A good fit was obtained for the three regions (I, II and III) and the values chosen for A_2 seem to be reasonable (see Section 4).

3.2. WC–Co alloy

Another example of the influence of temperature on the log σ versus log $\dot{\varepsilon}$ curves is shown in Fig. 3 for a WC–Co alloy with $d = 1.3\,\mu m$. Using the same procedure as above and the parameters in Table I, one obtains not only a good fit between the experimental data and the theoretical curves but also reasonable values for A_2.

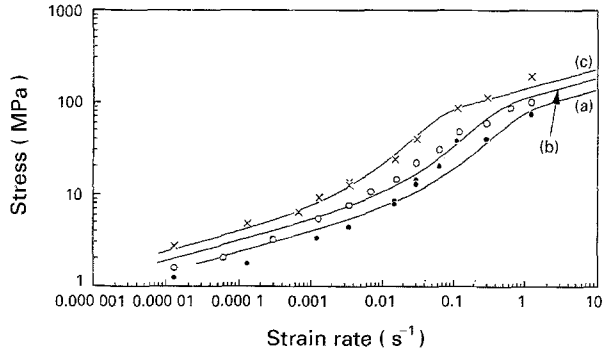

Figure 2 The log σ versus log $\dot{\varepsilon}$ curves of a Zn–22% Al alloy at various temperatures; experimental data points [17] are superposed on the fitted curves of the composite model. (a) ● 503 K, (b) (○) 473 K, (c) 423 K. $d = 2.5\,\mu m$.

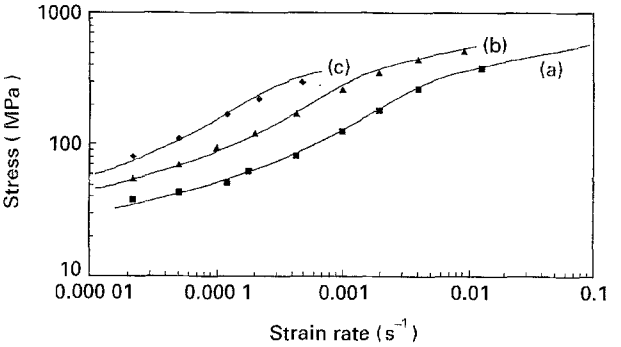

Figure 3 The log σ versus log $\dot{\varepsilon}$ curves of a WC–Co alloy at various temperatures; (■, ▲, ◆) experimental data points [18] are superposed on (——) the fitted curves of the composite model. (a) (■) 1200 °C, (b) (▲) 1150 °C, (c) (◆)1100 °C, $d = 1.3\,\mu m$.

TABLE I Parameters used in the stress versus strain-rate simulation with the composite model

Alloy	T (K)	Q_{gb} (kJ mol^{-1})	δD_{gb0} (m^3 s^{-1})	b (10^{-9} m)	A_1[a]	A_2[a]	n	F_{gb}
Zn–22% Al ($d = 2.5\,\mu m$) [17]	423–503	60[23]	1.9×10^{-14}[23]	0.27	1×10^{-10}	90–150	4.5	0.79
WC–Co ($d = 1.3\,\mu m$) [18]	1373–1473	460[18]	1×10^{-13}[23]	0.29	2×10^{-16}	920–1550	5	0.69
P/M Al–5Mg–Mn ($d = 1\,\mu m$) [19]	823	60.2[23]	1.9×10^{-14}[23]	0.286	2.17×10^{-7}	28	5	0.56
Al–alloy ($d = 0.5$–$15\,\mu m$) [20]	500	60.2[23]	1.9×10^{-14}[23]	0.286	3×10^{-8}	40	5	0.56

[a] A_1 and A_2 are expressed in international units.

TABLE II Parameter A_2 for Zn–22% Al and WC–Co at various temperatures

Alloy	$\dot{\varepsilon}$ (s^{-1})	T (K)	A_2^*	A_2(cal)[a]	A_2(fit)[a]	Q (kJ mol^{-1})	D_0[23] (m^2 s^{-1})
Zn–22% Al	1	423	1×10^4	158	150	60[23]	1.9×10^{-5}
(2.5 μm)	1	473	1×10^4	109	110	60[23]	1.9×10^{-5}
	1	503	1×10^4	90	90	60[23]	1.9×10^{-5}
WC–Co	0.01	1373	692	1570	1550	460[18]	1×10^{-4}
(1.3 μm)	0.01	1423	692	1191	1350	460[18]	1×10^{-4}
	0.01	1473	692	920	920	460[18]	1×10^{-4}

[a] A_2(fit) are the values used to fit the experimental log σ versus log $\dot{\varepsilon}$ curves and A_2(cal) are the values calculated from Equation 9a at various temperatures using a constant A_2^*. A_2^*, A_2(fit) and A_2(cal.) are expressed in international units.

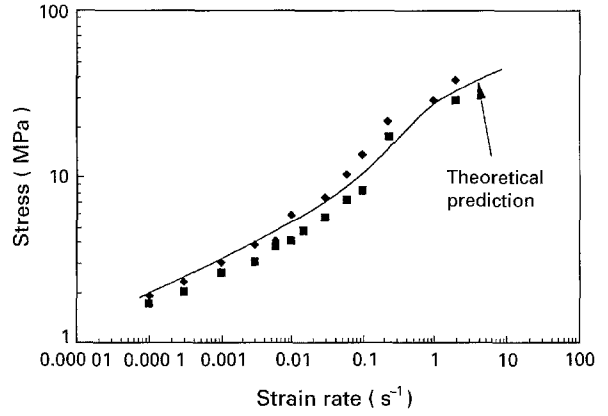

Figure 4 The log σ versus log ε̇ data of two P/M Al–5 Mg–Mn alloys with the fitted curve for the composite model. $T = 823$ K; (◆) 1.5 Mn, (■) 2.2 Mn.

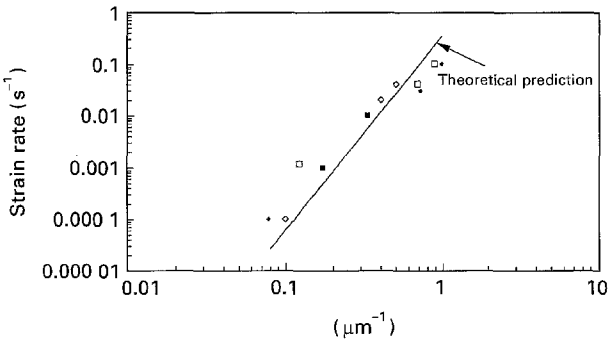

Figure 5 The optimum strain rate as a function of the reciprocal of grain size of P/M alloys. Optimum strain rate corresponds either to experimental maximum elongation or to the calculated maximum strain-rate sensitivity. (■) Al–5 Mg–Mn, (□) Al–5 Mg–Zr, (◆) Al–4.3 Cu–Zr, (◇) 7475 Al + Zr.

3.3. P/M Al alloys [16] and Al alloys [17]

Typical log σ versus log ε̇ data for two P/M Al-5Mg–Mn alloys [19] and the corresponding theoretical curve calculated with the parameters in Table I are plotted in Fig. 4. From the fitted behaviour, the strain rate corresponding to the maximum value of strain-rate sensitivity, m, can be calculated and this optimum value for the strain rate is compared to the experimental value for maximum elongation (Fig. 5) as a function of the reciprocal grain size. The theoretical curve describes the trend of experimental data fairly well and one obtains a grain size exponent of 3.

Another group of alloys can be considered. From the data for aluminium alloys with various grain sizes ranging from 0.5–15 μm [20], the same fitting procedure was done using the parameters in Table I. From the fitted curves, one can obtain values of the strain-rate sensitivity, m, which can be related to elongation through the simple relationship [21]

$$\text{Elongation (\%)} = \left[\left(\frac{m}{\Delta}\right)^{m} - 1\right] \times 100\% \quad \text{with } \Delta = 0.01 \qquad (11)$$

The experimental (Fig. 6a) and calculated (Fig. 6b) variations of elongation as a function of strain rate can now be compared. In both, the presence of high strain-rate superplasticity is clearly seen. The calculated elongation peaks at optimum strain rates are

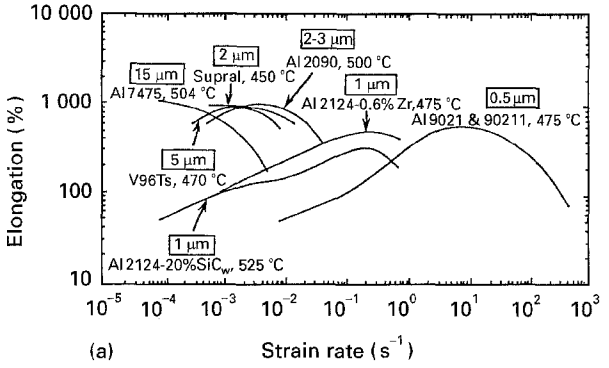

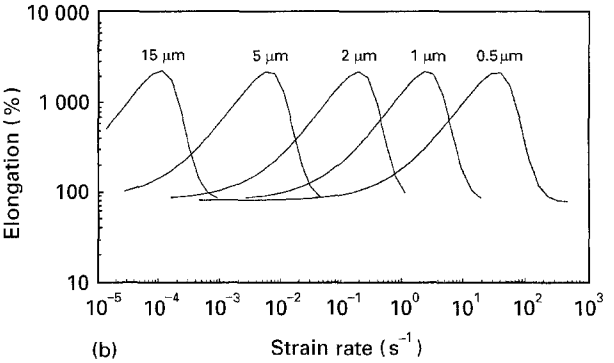

Figure 6 (a) Experimental curves of elongation to failure as a function of strain rate for various aluminium alloys [20] having diferent grain sizes. (b) Elongation to failure as a function of strain rate for aluminium alloys calculated with the present composite model for different grain sizes, at 500 °C.

higher than those experimentally observed and this may be due to the occurrence of cavitation [22]. Although good fits have not been obtained, the model can show the general tendency of the influence of grain size on the behaviour of elongation versus strain rate and, in particular, the high strain-rate plasticity for grain sizes less than 1 μm. To obtain good fits, one must introduce material-dependent A_1, A_2 and F_{gb} parameters, i.e. different values for different aluminium alloys.

4. Discussion

In the above calculation, the parameter F_{gb}, which approximately reflects that part of optimum superplastic strain rate due to grain-boundary sliding and which was chosen between 0.56 and 0.79, was found to have a dominant influence on both the strain-rate range for region II and the maximum value of the strain-rate sensitivity. Fig. 7 shows the maximum m value as a function of F_{gb} for P/M aluminium alloys calculated with the composite model. This m value increases with F_{gb}, reaching $m = 1$ for pure GBS. For a typical m value of 0.5, F_{gb} is equal to 0.6; this agrees with the reported (~ 60%) contribution of GBS in the total strain [2, 24].

The parameter A_2 may be found either by simply fitting Equation 9b to the experimental data for each test temperature, or by obtaining A_2^* from a fit of Equation 9a at one test temperature and calculating the value of A_2 for all other temperatures. For both Zn–22% Al and WC–Co alloys, these two procedures

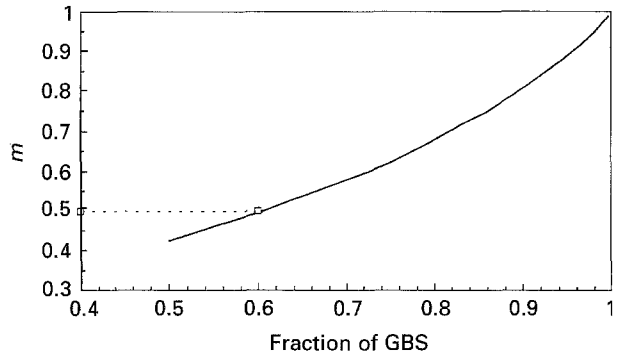

Figure 7 Strain-rate sensitivity, m, as a function of F_{gb} calculated with the composite model using parameter values for P/M aluminium alloys.

lead to similar values for A_2 if the activation energy is taken to be that for grain-boundary diffusion, i.e. the same values as those for region II (see Table II). It therefore seems that in these two small-grained materials, the dislocation creep mechanism may be controlled by grain-boundary diffusion, or by dislocation pipe diffusion whose activation energy is of similar magnitude. This observation does not agree with the usual assumption that dislocation creep in region III is dominated by volume diffusion (see the review paper by Kashyap and Mukherjee [25]).

Experimental data [1, 2] and theoretical models [3–9, 25], usually consider the value of the grain-size exponent, p, to be around 2–3. In the present model, this value, found to be equal to 3, falls within this range. However, it must be noted that the value that p takes depends on how it is defined. In Figs 5 and 6, where it is defined for the optimum strain rate, a value of 3 is obtained. However, if the exponent is measured for a constant stress in region II, it varies in the range of about 2.2–2.6, depending on the stress levels and on the parameter values assumed.

Finally, for the behaviour described in the present model, strain rates must neither be too low nor too high. At too low strain rates, GBS stress levels are much lower than the intragranular creep flow stress and the deformation behaviour is comparable to that of glass marbles immersed in a connected fluid; the deformation is then controlled by the behaviour of the fluid (m high). At too high strain rates, GBS stress levels are much higher than the intragranular creep flow stress; the deformation behaviour can then be considered similar to that of highly deformable marbles surrounded by a less deformable connected phase and this behaviour will be controlled by the latter (m high) (Fig. 8). The extent of the strain-rate range in which the model is applicable should depend on the thickness of the connected phase because one must expect the "extreme" strain-rate ranges (too low or too high) to move towards each other as the connected phase becomes thicker. These qualitative observations are in agreement with the theoretical approach based on the theory of di-phased material homogenization [26].

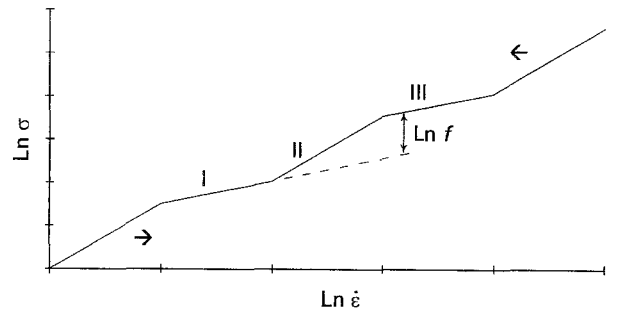

Figure 8 Schematic representation of the stress, σ, as a function of strain rate, ε̇, showing the regions of applicability of the composite model (regions, I, II and III) as well as the regions of too low or too high strain rates: the arrows indicate the displacement direction of the latter two regions as the fraction of the connected phase increases.

5. Conclusion

1. A composite model for superplastic deformation is proposed based on the Baudelet and Ashby–Verrall models.

2. The composite model takes into account grain-boundary sliding and dislocation creep and can describe the stress versus strain-rate behaviour for a number of superplastic materials. The influence of temperature and grain size on the $\log \sigma$ versus $\log \dot{\varepsilon}$ curve can also be predicted.

References

1. J. W. EDINGTON, K. N. MELTON and C. P. CULTER, *Prog. Mater. Sci.* **21** (1976) 61.
2. J. W. EDINGTON, *Metall. Trans.* **13A** (1982) 703.
3. M. F. ASHBY and R. A. VERRALL, *Acta Metall.* **21** (1973) 149.
4. A. BALL and M. M. HUTCHINSON, *Metal Sci. J.* **3** (1969) 1.
5. A. K. MUKHERJEE, *Mater. Sci. Eng.* **8** (1971) 83.
6. J. R. SPINGARN and W. D. NIX, *Acta Metall.* **27** (1979) 171.
7. R. RAJ and M. F. ASHBY, *Metall. Trans.* **2A** (1971) 1113.
8. R. C. GIFKINS, *ibid.* **7A** (1976) 1225.
9. H. W. HAYDEN, S. FLOREEN and P. D. GOODELL, *ibid.* **3** (1972) 833.
10. E. W. HART, *Acta Metall.* **15** (1967) 1545.
11. F. W. CROSSMAN and M. F. ASHBY, *ibid.* **23** (1975) 423.
12. F. GHAHREMANI, *Int. J. Solids Struct.* **16** (1980) 847.
13. B. BAUDELET, *Scripta Metall. Mater.* **27** (1992) 745.
14. P. M. HAZZLEDINE and D. E. NEWBURY, in "Proceedings of ICSMA3" (Institute of Metals, London, 1973) p. 202.
15. D. S. DARMAID, A. W. BOWEN and P. G. PARTRIDGE, *J. Mater. Sci.* **19** (1984) 2378.
16. M. G. ZELIN and M. V. ALEXSANDROVA, in "Superplasticity in Advanced Materials", edited by S. Hori, M. Tokizane and N. Furushiro (JSRS, Osaka, Japan, 1991) p. 63.
17. F. A. MOHAMED, M. M. I. AHMED and T. G. LANGDON, *Metall. Trans.* **8A** (1977) 933.
18. T. SAKUMA and H. HONDO, in "Superplasticity in Advanced Materials", edited by S. Hori, M. Tokizare and N. Furushiro (JSRS, Osaka, Japan, 1991) p. 349.
19. K. HIGASHI, S. ITSUMI, M. HOSHIKAMA, Y. MATSUMURA, T. ITO, S. TANIMURA and H. YOSHIDA, *ibid.*, p. 575.
20. T. G. NIEH and J. WADSWORTH, *ibid.*, p. 339.
21. J. LIAN and B. BAUDELET, *Mater. Sci. Eng.* **84** (1986) 157.
22. J. LIAN and M. SUERY, *Mater. Sci Technol.* **2** (1986) 1093.
23. I. KAUR, W. GUST and L. KOZMA, in "Handbook of Grain and Interphase Boundary Diffusion Data", Vols 1 and 2 (Ziegler Press, Stuttgart, 1989), pp. 118, 1400, 1403, 1416.
24. D. HOLT, *Trans. TMS-AIME* **242** (1968) 25.
25. B. P. KASHYAP and A. K. MUKHERJEE, in "Superplasticity", edited by B. Baudelet and M. Suery (CNRS, Paris, 1985) p. 4.1.
26. R. DENDIEVEL, private communication.

Received 29 April
and accepted 27 July 1994